

## Effect of Phosphate Conversion Coating Containing Cobalt Ion on the Corrosion Resistance of 6061 Aluminum Alloy

H Zarei<sup>1</sup> and R Hosseini Rad<sup>2\*</sup>

<sup>1</sup>Graduate Center, Department of Materials Engineering, Shahid Sattari Aeronautical University of Science and Technology, Tehran, Iran

<sup>2</sup>Faculty of Engineering, Tarbiat Modares University, Tehran, Iran

\*Corresponding author: R Hosseini Rad, Faculty of Engineering, Tarbiat Modares University, Tehran, Iran, Tel: +254721857685; E-mail: rad.reza1371@rocketmail.com

Received: January 17, 2018; Accepted: March 02, 2018; Published: March 09, 2018

### Abstract

Corrosion properties and phase analysis of zinc phosphate conversion coating (ZPCC) formed on the T6-6061 aluminum alloys, after immersion in phosphating bath containing various amounts of  $\text{Co}^{+2}$  (0, 5, 9, 13 g/L), was investigated by the mean of scanning electron microscope (SEM), electrochemical spectroscopy impedance (EIS) and potentiodynamic polarization technics (Tofl plots). Results showed that with increase in cobalt ion concentration to 9 g/L, crystals size reduced and pores on the surface decreased to lowest amount. So that impedance module of sample which is containing 9 g/L of cobalt ion, is almost 4 and 2 times greater than the pure sample and that which is containing 5 g/L of cobalt ions, respectively. Moreover, results of potentiodynamic polarization showed that incrimination of cobalt ion dosage lead to both decrease corrosion current density and shifts potential to positive amounts.

**Keywords:** Zinc phosphate; Conversion coating; Spectroscopy; Impedance; Polarization; Scanning electron microscope; Corrosion

### Introduction

Aluminum alloys, are used widely in aerospace industries due to their high strength to weight ratio. However, low corrosion resistance could be mentioned as a drawback for the aluminum applications. One of the common methods to enhance aluminum's corrosion resistance is utilizing conversion coating that are employed in aerospace industries and airplanes on the aluminum substrates. These coatings apart from decorating cause to improve corrosion resistance. This coating system comprises of a conversion coating as a primer, utilized to enhance the adhesion of the top coat to the substrate and a top coat. In this system, top coating can be epoxy matrix resins with hardening agents made from amines or polyamides [1,2].

Corrosion inhibitors such as strontium chromate, usually add to primer or first coating to increase corrosion resistance. Epoxies commonly are employing as the top coat in aerospace coating systems [2].

Conversion coating treatment on the surface of the metal is one of the prevalent methods that increase the corrosion resistance [3-7]. Compared with another methods of coating, such as anodizing [8], electroplating [9], electrolysis plating [10], physical vapor deposition [11], sol-gel [12], chemical treatment is one of the most effective methods of surface preparation that has noteworthy advantages, for instances facility and low cost of coating operation[13,14].

Chromate, anodized and zinc phosphate coatings can be noted as the conversion coatings [15]. Zinc phosphate coatings are used for many years as primer to increase adhesion of paints on the substrates of steel and aluminum [16-19]. Although conversion coatings have high corrosion resistance, utilizing Cr (VI) is confined because of toxicity issues [20]. ZPCC is one of most attractive chemical conversion coating methods that commonly is substituted as a primer coating on the steel and aluminum alloys, instead of chromate conversion coatings due to several advantages, such as low preparation cost, environmentally friendly and simplicity of operation [15].

Conversion coating process has electrochemical nature that starts with destroying oxides on the surface of the metal with the hand of an acidic solution. Nevertheless, electrolyte contacts with the metal surface directly so that during phosphate operation on the aluminum, following reactions occur.



Solving aluminum in anodic local sites causes both  $\text{H}^+$  concentration decreases and finally increasing pH lead to shift the reaction (2b) to the right and prepare suitable condition to deposition of zinc phosphate (ZPO) [20]. The aim of adding additives to the phosphate bath is to modify coating characteristics. For example F- usually add to phosphate bath to increase etching rate and limiting free  $\text{Al}^{3+}$  ions in solution, because  $\text{Al}^{3+}$  has distracting effects on the growth of coating [21].

In order to achieve high quality phosphate coatings, several investigations have been done around the enhancing quality of coatings through utilizing nickel and manganese ions [22-25]. It Has been shown that adding metallic salts to phosphating bath has significant effects on the structure of zinc coating in a way that makes it smaller and denser[26]. Adding  $\text{Co}^{2+}$  to the phosphating bath would increase corrosion resistance of the ZPO coating applied on the [21,26]. Furthermore, it has been reported that adding  $\text{Ni}^{2+}$  to the phosphating, bath improves corrosion resistance of ZPO coatings applied on the aluminium-2024 alloys [23]. Bajat et al. discovered that phosphate coating applied on the galvanized steel increased the adhesion strength of organic coating. Deflorian et al. reported that chromate conversion coating improved significantly the adhesion

strength of organic coatings. The influence of surface pretreatment on the steel by zirconium conversion coating on the adhesion performance and the cathodic delamination of epoxy coatings was evaluated by Ghanbari et al. and it was shown that surface pretreatment increased the barrier properties, cathodic disbondment resistance and adhesion strength of epoxy coatings.

The main aim of this study was investigating the effect of ZPCCs and cobalt ions in the phosphating bath, on the corrosion resistance of aluminum T6-6061. Actually in this study the main goal is to change the zinc phosphate coating's surface by adding different amounts of cobalt ion to the phosphate bath that is expected to improve corrosion properties of zinc phosphate coating, because it is thought that the addition of cobalt ions can reduce the porosity and imperfections on the surface of the coating. In order to investigate the influence of cobalt ion on the formed coatings on the aluminum samples SEM, EIS and potentiodynamic polarization techniques, were employed. The method of approach is in a such way that first the change in the surface of coating will be approved by SEM images, then the effect of this change on corrosion properties of zinc phosphate coating will be analyzed by EIS and potentiodynamic polarization techniques, it is also valuable to be mentioned that electrochemical impedance spectroscopy is one of the most powerful method for investigating corrosion properties of coatings, which has been rarely used in similar works. In recent studies cobalt has been used gradually as additive in phosphate bath.

Results showed that with increase cobalt ion amount to 9 g/L, crystals size reduce and surface porosity decreases to lowest amount. So that impedance module of sample which is containing 9 g/L of cobalt ion, is almost 4 and 2 times greater than the pure sample and that which is containing 5 g/L of cobalt ions, respectively. Moreover, results of potentiodynamic polarization showed that increasing cobalt ion concentration; tend to both decrease corrosion current density and shifts potential to positive amounts.

## Materials and Methods

### Materials

TABLE 1. Chemical composition of 6061-T6 Al.

Element	Silicon	Cobalt	Copper	Manganese	Cobalt	Chrome	Zinc	Titanium	Aluminum	Other
Component amount (Wt%)	0.4-0.8	0.7	0.15-0.4	0.15	0.8-1.2	0.04-0.35	0.25	0.15	95.85-98.56	0.15

### Preparation of substrate and phosphate coating treatment

Aluminum samples with dimension of  $150 \times 50 \times 1$  mm were sanded until 2000 grade. The corner of sample was accurately sanded due to accumulation of electrical charge. After sanding, the samples were washed with deionized water and then were degreased in 25% NaOH solution for 3 minutes and washed in deionized water again. After that, samples were pickled in 20% Nitric acid for 4 minutes. After preparation, samples were immersed in phosphating bath, which containing various concentration of cobalt ions. pH adjustment was done by adding NaOH to the electrolyte. The composition of used bath for phosphating treatment is presented in TABLES 1 and 2. The phosphating temperature was  $85^{\circ}\text{C}$ , treatment time was also 30 min and the pH of the bath was about 2.5. In order to investigate the impact of cobalt ion concentration on the coating properties, different concentrations of cobalt ions was added to phosphating bath.

TABLE 2. Phosphating bath composition A) Without addition B) Containing cobalt (II) nitrate.

Chemical compound	A	B
H <sub>3</sub> PO <sub>4</sub> (ml/L)	9	9
HNO <sub>3</sub> (ml/L)	2.5	2.5
ZNO(g/L)	5.6	5.6
NaNO <sub>2</sub> (g/L)	1	1
NaF(g/L)	0.3	0.3
Mg(NO <sub>3</sub> ) <sub>2</sub>	-	5-3

### Microstructure and composition of coating

Surface morphology of the coating was analyzed by the mean of scanning electron microscopy (Philips-XL30) and also composition of fabricated coating was characterized using X-ray diffraction method (XRD) with Co K $\alpha$  radiation at 40 kW and a scanning speed of 100/min.

### Corrosion resistance evaluation

Corrosion behavior of the fabricated coating at various concentrations of Co ions were evaluated using potentiodynamic polarization and EIS tests (EG&G model parstat 2263). All of experiments were done in three electrode cells, in which saturated calomel electrode (SCE) were employed as reference electrode. A platinum plate served as counter electrode and 1 cm<sup>2</sup> of substrate served as working electrode. EIS test was carried out after 1, 3, 7, 14, 21 and 28 days immersion in 3.5% NaCl solution and then, potentiodynamic polarization test was performed after EIS test. The EIS data were recorded at the OCP (open circuit potential) with a sinusoidal perturbation of 10 mV amplitude over the frequency range from 10-2 Hz to 105 Hz. The polarization measurements were scanned from – 250 mV (relative to the OCP) to +250 mV (relative to the OCP) at a scan rate of 1 mV/s. the data were obtained by Powersuit software and finally bode and nyquist plot were analyzed using zviw2.

## Results and Discussion

### Phase analysis, microstructure and mechanism of action of cobalt ion on the forming of coating

X-ray diffraction spectra of the samples coated in various dosages of cobalt ions has been displayed in FIG. 1. As it can be seen, most important phase in the composition of phosphate coating, is Hopeite phase, which has been noted in the recent researches around the phosphate bath coating as well [27-29]. In addition to Hopeite phase, Phosphophyllite is also may observe in X-ray diffraction spectrum in the ZPO coatings applied on the steel [30,31]. Despite Hopeite phase aluminum can be seen in x-ray diffraction that can be related to the low thickness of the phosphate coating (around 7 microns) formed on samples. Since X-ray can penetrate deep up to 15 microns, so that is whray has detected aluminum substrate.

SEM results of the samples coated in different concentrations of cobalt ions has shown in FIG. 2, as well as samples coated in phosphating bath without cobalt ions. As it can be shown, the morphology of the phosphate crystals is flower-like and plate-like. It is generally accepted that flower-like and plate-like crystals and needle-shaped crystals are characteristics related to Hopeite crystals (Zn<sub>3</sub>(PO<sub>4</sub>)<sub>2</sub>·4H<sub>2</sub>O) and Phosphophyllite crystals respectively [32]. It is possible to observe needle-shaped

crystals in zinc-cobalt phosphate baths [33] and zinc phosphate bath as well [34,35]. These phases were also observed in X-ray diffraction spectra of the samples. As it shown in FIG. 2, the cobalt ions in the coating bath have significant effect on the coating morphology in a way that, coating formed in the bath without cobalt ions, has higher porosity, the surface has not covered completely by the crystals and crystals did not adhere to the surface properly. As it can be seen, with increasing cobalt ions concentration in coating bath, the surface porosity has decreased and the coating has become denser. With further incriminations in concentrations more than 9g/L (FIG. 2), it was observed that almost, the surface has covered completely by phosphate coating crystals and approximately no rough porosity detected on the surface.

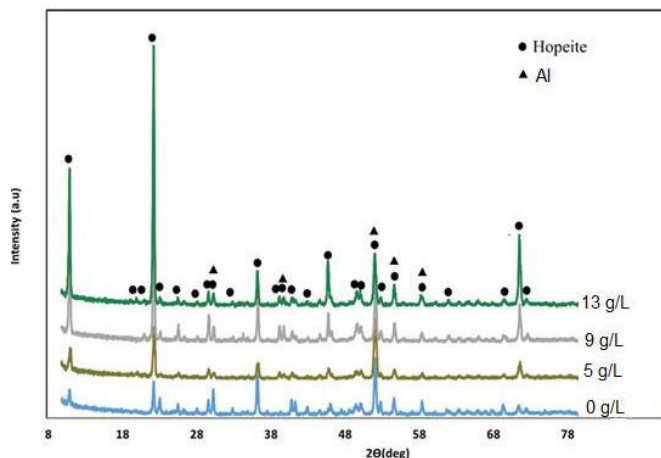


FIG. 1. The spectrum of the X-ray diffraction for phosphate coatings containing different amounts of cobalt ions.

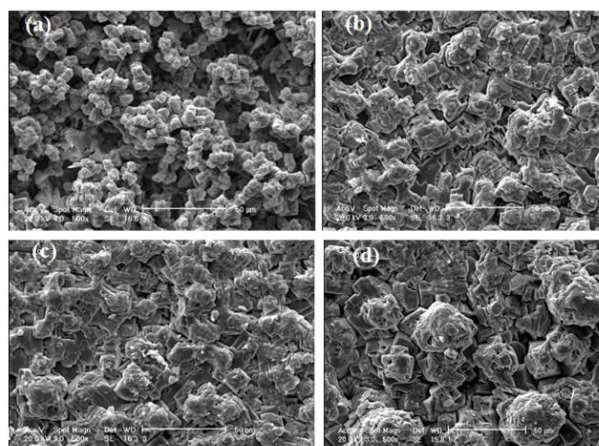


FIG. 2. Scanning electron micrographs of phosphate conversion coatings containing different amounts of cobalt formed a) without cobalt ion b) 5g/L c) 9g/L d) 13 g/L.

This can affect impressively on the corrosion resistance of coatings. When the metal substrate with lower standard electrode potential immersed in a solution containing cations with higher standard electrode potential, the more Nobel metal could reduce spontaneously on the metal with more negative electrode potential. In this case reduction potentials and reactions of cobalt and aluminum ions are represented as follows:





Standard reduction potential of cobalt and aluminum are -0.28 and -1.66 respectively, so they can react through following reaction:



According equation 6 substrate dissolve easier, so that forming Hopeite would accelerate. As it can be observed in FIG. 1, with increasing concentration of cobalt ions of the coating bath, the peak height of X-ray diffraction spectra has increased; this can be related to the acceleration of the coating growth. A similar mechanism around impact the cobalt ions on the nucleation of Hopeite in galvanized steel phosphating have proposed by Yu Su et al. They also considered that with addition cobalt ions to the phosphate coating bath, the coating porosity on the galvanized steel will decrease, that can be relevant to more positive reduction potential of cobalt than that of zinc. Cobalt ions could tend to form thinner coatings, because it has proven that coatings formed in the phosphating baths containing cobalt and manganese are thinner than those of which formed without additives [18,21]. The rate of increasing solution pH at the alloy surface is slowed down powerfully by the sluggish solution kinetics of  $\text{Ni}^{2+}$  and  $\text{Mn}^{2+}$  ions than that by the  $\text{Co}^{+2}$  (verified experimentally), which lead to decline precipitation and form thinner coatings [36].

### Electrochemical impedance spectroscopy (EIS)

EIS method is used for evaluating the corrosion resistance [37]. This method shows the changes in the metal-coating interface in shorter times than conventional methods and results recorded from EIS provide comprehensive information about coatings [38]. The corrosion process usually starts with saturation of coating by water available in corrosive environment and ends with accumulation of corrosion products at the coating-substrate interface [37]. As it is shown, there are two semi-circle in high and medium frequency ranges for capacitor and a semi-circle in low frequency range for inductor in the Nyquist plots of the samples. In some cases, it is difficult to distinguish semi-circles related to capacitor and even in some times in low frequencies, inductor semi-circle is not clear. However, the most accurate data fitting with the minimum error (chi-square), with two time constants is suggested using the equivalent circuit based on Nyquist plots and EIS studies and researches of Duan et al. [39], Ghasmi et al. [40] (FIG. 3 and FIG. 4). In the suggested equivalent circuit,  $R_e$ , CPE1-R1, CPE2-R2 represents the electrolyte solution resistance, the constant phase element (due to the semi-circle bruise) phosphate coating resistance represent the constant phase element and the resistance of double layer respectively [41].

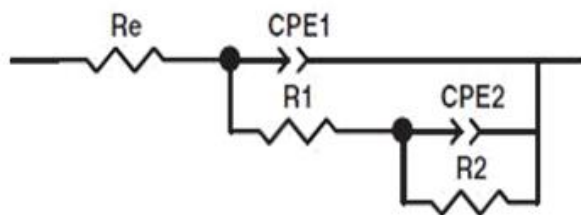


FIG. 3. Proposed equivalent circuit for fitting impedance data.

To obtain data fit that is more accurate and to consider roughness factor, the constant phase element is used instead of accurate capacitive element, so the impedance of constant phase element (CPE) can be described by the following formula:

$$Z_{CPE} = 1/T(j\omega)^P$$

In which T is CPE constant,  $\omega$  is angular frequency (radian per second) and P is a variable changes between 0 and 1, so that if P=1, equation 1 equals to the impedance of the net capacitor and if P=0, it equals to the impedance of pure resistance [42].

To examine the impedance data precisely, the values of constant phase element can be converted to capacitive capacitance through the following formulation:

$$C = (CPE \cdot R)^{1/n} / R$$

In which, C, CPE, R, n represent are capacitance, constant phase element, resistance and exponential power respectively [43]. In FIG. 5, the graph of extracted data from the described model in FIG. 3 is plotted vs. time. FIG. 5, state that R1 (phosphate coating resistance) is lower than R2 (double layer resistance). Decrease in R1 and R2 can attributed to penetrating corrosive solution through available pores of the coating and reaching to the substrate and then corroding it (5a, 5c), which gradually reduces the protective properties of coating [40]. However, it is possible that corrosion products over immersion time produce and fill the pores and cracks. Consequently, penetration of the electrolyte to the substrate is restricted and corrosion resistance would increase (5a, sample 1, 3, 4). It was observed that corrosion resistance declined again after 3 days. This can contribute to dissolving corrosion products and diffusion of electrolyte into the coating again. There are two semi-circles in FIG. 4 (the Nyquist plots) for all the samples, high frequencies and a low frequencies curve. Semi-circle related to the high frequencies represents corrosion properties of the first layer (porous layer), while that of related to the low frequencies, shows the corrosion properties of barrier layer that are denser than surface layer. Consequently, the higher differences of curves (FIG. 4) at low frequencies in various immersion times are because of that the lower frequencies show the properties of inner part, which is close to the substrate and is denser than surface layer whereas high frequency's curve displays properties of outer layer which is far from substrate [39].

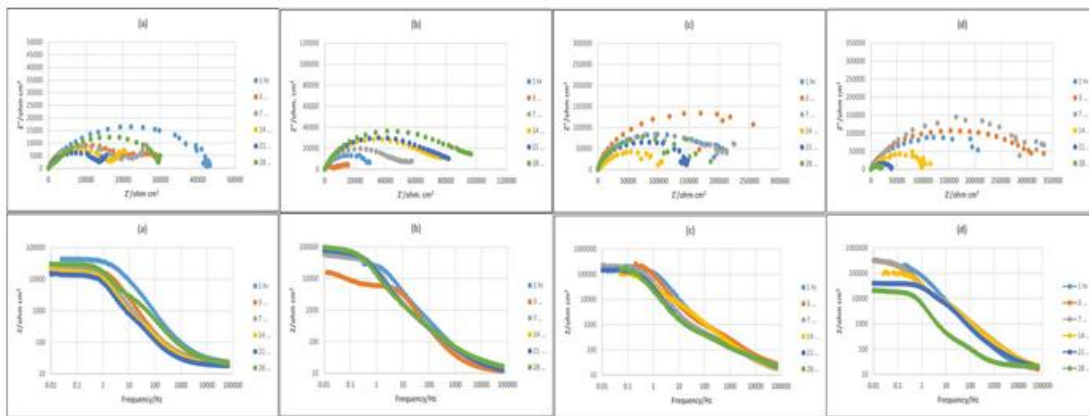


FIG. 4. Bode and Nyquist plots related to a) without ion b) 5g/L cobalt ion c) 9g/L d) 13g/L in different immersion times (1, 3, 7, 14, 21, 28 hours) in the 3.5%NaCl.

With increasing immersion time, radius of high frequencies semi-circle would decline. As it can be seen in FIG. 4, the semi-circle related to low frequencies, suggests that electrochemical reactions are progressing in the metal-coating interface. In other word in this stage, the diffusion through pores has accomplished and electrolyte contacts with metal-coating interface and corrosion cell is activated [44]. However, the second semi-circle radius of low frequencies has decreased, which shows an increment in the rate of corrosion through the creation and production of newer porosities, or to the increase in porosity and surface defects in coating [41]. Accordingly, the metal surface is completely covered. SEM results (FIG. 2) show that the surface of samples coated in phosphating bath, containing higher amounts of cobalt ions (9 and 13 g/L), are denser, have lower porosities and penetration within the pores towards the substrate is labored as well (4c, 4d). Increasing concentration of cobalt ions up to 9 g/L changes the morphology of coatings, in a way that make them denser and minimize the diffusion of electrolyte. Accordingly, impedance and corrosions resistance rise up to 10 times higher than the samples coated in bathes with lower cobalt ions dosage (FIG. 5a and 5c). FIG. 5 shows corrosion resistance changes of coating vs. time. Three Time regions are available in the FIG. 5, which represent different stage of the penetration of electrolyte through coating. Rcoat usually decreases over time owing to entrance of electrolyte into the coating. As it is shown in FIG. 5, for example, the coating resistance of sample 4 decreases from  $8e4$  to  $6e4$  ohm.cm<sup>2</sup>. In the next stage the resistance increases, because corrosion products would fill porosities and finally for long time of immersion, coating resistance decreases, due to diffusion of deionized water and chloride ions to the substrate-coating interface [45]. SEM results and impedance data of samples, show that increasing cobalt ion concentration decrease coatings porosity. Capacitance is one of the important parameters to measure the amount of water penetrated into the coating pores. Coating capacity is affected by penetration of electrolyte and corrosive ions into the coating pores, in a way that when the volume of defects and voids in the coating is large, capacity of coating would increase significantly over long exposure time. In some cases, after short immersion time in saline environment, coating capacity once increased and after a while decreased, that can attribute to the filling of defects by produced corrosion products (5b, 5d). It was observed that the increment of c1 in the early days of immersion is more than c2, owing to the porous structure of the surface layer, which diffusing electrolyte through and after a while, capacity has fallen more, because of blockage of pores by corrosion products. In the end times of immersion, when the coating is saturated with water and electrolytes, coating capacity stabilizes [46].

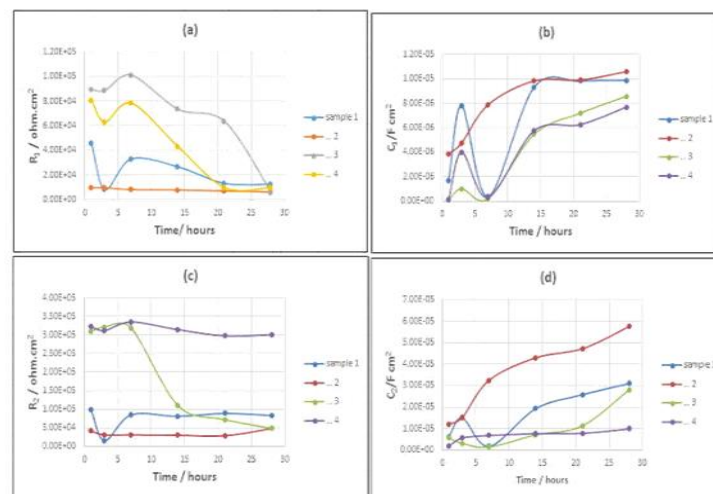


FIG. 5. Parameters resulted from fitting impedance data vs. immersion time A) phosphate coating resistance (R1) B) capacity of surface layer (C1) C) double layer resistance (R2) D) capacity of inner part of phosphate coating (C2).

In order to evaluate the effect of cobalt ion on the corrosion of coated samples, potentiodynamic polarization test was performed after 28 hours of immersion. FIG. 6 shows the influence of cobalt ions. As it seen, samples coated in bath without cobalt ions have potentials that are more negative, whereas by addition cobalt ion to the phosphating bath, the potential of samples is shifted toward positive values. This can contribute to decline in the cathodic reaction rate by increasing cobalt ions. As it mentioned before coating covers the surface completely and blocks the diffusion of corrosive species within pores and increases their number that tends to decrease corrosion, but further increment of cobalt ions up to 13g/L to the phosphating bath, have no further effects (FIG. 6). As it is shown the potential of both samples are same, that current density would decrease by raising cobalt ion concentration. It has proven that conversion coatings lead to change in anodic curve, while cathodic one does not change. This states that conversion coatings reduce the rate of anodic reaction more than cathodic one [47].

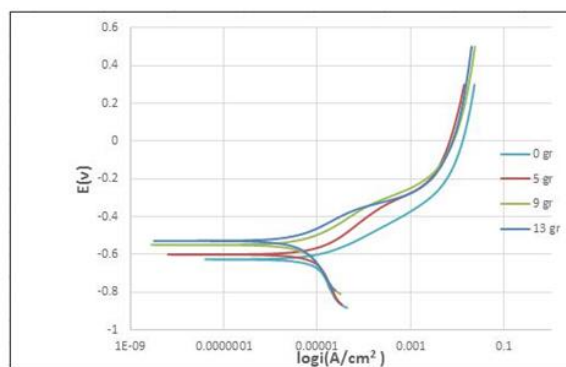


FIG. 6. Potentiodynamic polarization curves of the samples treated to the zinc phosphate solution at pH=2.5, T=85 C, t=10 min in different amounts of  $\text{Co}^{2+}$  (0, 5, 9, 13 g/L) after 28 h. of immersion in the NaCl 3.5%.

## Conclusions

- 1- Using of phosphate conversion coating as primer improves corrosion resistance of aluminum alloy.
- 2- Adding 9 g/L of cobalt ions to the phosphate bath would impressively decrease surface porosities of phosphate coating.
- 3- The 9 g/L of cobalt ion enhance corrosion resistance of aluminum owing to accelerate in growth of hopeiet crystals.
- 4- Increment in dosage of cobalt ions up to 13 g/L has not significant effect on improvement of corrosion resistance of aluminum.
- 5- The EIS results also show that by adding cobalt ion up 9 g/L to the phosphate bath, the impedance module has increased roughly 9 times than phosphate coating without ion one.

## REFERENCES

1. Osborne JH. Observations on chromate conversion coatings from a sol-gel perspective. Prog Org Coat. 2001;41(4):280-6.
2. Du YJ, Damron M, Tang G, et al. Inorganic/organic hybrid coatings for aircraft aluminum alloy substrates. Prog Org Coat. 2001;41(4):226-32.

3. Chen J, Song Y, Shan D, et al. Study of the *in situ* growth mechanism of Mg-Al hydrotalcite conversion film on AZ31 magnesium alloy. *Corros Sci.* 2012;63:148-58.
4. Li Q, Xu S, Hu J, et al. The effects to the structure and electrochemical behavior of zinc phosphate conversion coatings with ethanolamine on magnesium alloy AZ91D. *Electrochim Acta.* 2010;55(3):887-94.
5. Guo KW. A review of magnesium/magnesium alloys corrosion and its protection. *Recent Patents on Corrosion Science.* 2010.
6. Hu RG, Zhang S, Bu JF et al. Recent progress in corrosion protection of magnesium alloys by organic coatings. *Prog Org Coat.* 2012;73(2-3):129-41.
7. Cui XJ, Liu CH, Yang RS, et al. Duplex-layered manganese phosphate conversion coating on AZ31 Mg alloy and its initial formation mechanism. *Corros Sci.* 2013;76:474-85.
8. Wang X, Zhu L, He X, et al. Effect of cerium additive on aluminum-based chemical conversion coating on AZ91D magnesium alloy. *Appl Surf Sci.* 2013;280:467-73.
9. Taha MA, El-Mahallawy NA, Hammouda RM, et al. PVD coating of Mg-AZ31 by thin layer of Al and Al-Si. *J Coat Technol Res.* 2010;7(6):793-800.
10. Liu Z, Gao W. Electroless nickel plating on AZ91 Mg alloy substrate. *Surf Coat Technol.* 2006;200(16-17):5087-93.
11. Zhou C, Xu J, Jiang S. Reactive sputter deposition of alumina films on magnesium alloy by double cathode glow-discharge plasma technique. *Mater Charact.* 2010;61(2):249-56.
12. Barranco V, Carmona N, Galván JC, et al. Electrochemical study of tailored sol-gel thin films as pre-treatment prior to organic coating for AZ91 magnesium alloy. *Prog Org Coat.* 2010;68(4):347-55.
13. Ramezanzadeh B, Attar MM. Evaluation of the effects of surface treatments on the cathodic delamination and anticorrosion performance of an epoxy-nanocomposite on steel substrate. *J Coat Technol Res.* 2013;10(1):47-55.
14. Chen XB, Birbilis N, Abbott TB. Effect of  $[Ca^{2+}]$  and  $[PO_4^{3-}]$  levels on the formation of calcium phosphate conversion coatings on die-cast magnesium alloy AZ91D. *Corros Sci.* 2012;55:226-32.
15. Van Phuong N, Moon S. Comparative corrosion study of zinc phosphate and magnesium phosphate conversion coatings on AZ31 Mg alloy. *Mater Lett.* 2014;122:341-4.

16. Sun X, Susac D, Li R, et al. Some observations for effects of copper on zinc phosphate conversion coatings on aluminum surfaces. *Surf Coat Technol.* 2002;155(1):46-50.
17. Zimmermann D, Munoz AG, Schultze JW. Microscopic local elements in the phosphating process. *Electrochim Acta.* 2003;48(20-22):3267-77.
18. Akhtar AS, Susac D, Wong PC, et al. The effect of pH and role of  $Ni^{2+}$  in zinc phosphating of 2024-Al alloy: Part II: Microscopic studies with SEM and SAM. *Appl Surf Sci.* 2006;253(2):502-9.
19. Lim JW, Lee JJ, Ahn H, et al. Mechanical properties of TiN/TiB<sub>2</sub> multilayers deposited by plasma enhanced chemical vapor deposition. *Surf Coat Technol.* 2003;174:720-4.
20. Gray J, Luan B. Protective coatings on magnesium and its alloys: A critical review. *J Alloys Compd.* 2002;336(1-2):88-113.
21. Akhtar AS, Wong KC, Wong PC, et al. Effect of  $Mn^{2+}$  additive on the zinc phosphating of 2024-Al alloy. *Thin Solid Films.* 2007;515(20-21):7899-905.
22. Oh JE, Kim YH. The corrosion resistance characteristics of Ni, Mn and Zn phosphates in automotive body panel coatings. *Ind Eng Chem Res.* 2012;18(3):1082-7.
23. Akhtar AS, Susac D, Glaze P, et al. The effect of  $Ni^{2+}$  on zinc phosphating of 2024-T3 Al alloy. *Surf Coat Technol.* 2004;187(2-3):208-15.
24. Flis J, Mankowski J, Zakroczymski T, et al. The formation of phosphate coatings on nitride stainless steel. *Corros Sci.* 2001;43(9):1711–25.
25. Sinha PK, Feser R. Phosphate coating on steel surfaces by an electrochemical method. *Surf Coat Technol.* 2002;161(2-3):158-68.
26. Tamilselvi M, Kamaraj P, Arthanareeswari M, et al. Nano zinc phosphate coatings for enhanced corrosion resistance of mild steel. *Appl Surf Sci.* 2015 Feb 1;327:218-25.
27. Darband GB, Afshar A, Aliabadi A. Zn-Ni Electrophosphating on galvanized steel using cathodic and anodic electrochemical methods. *Surf Coat Technol.* 2016;306:497-505.
28. Jegannathan S, Arumugam TK, Sankara Narayanan TSN, et al. Formation and characteristics of zinc phosphate coatings obtained by electrochemical treatment: Cathodic vs. anodic. *Prog Org Coat.* 2009;65(2):229-36.
29. Simescu F, Idrissi H. Corrosion behaviour in alkaline medium of zinc phosphate coated steel obtained by cathodic electrochemical treatment. *Corros Sci.* 2009;51(4):833-40.

30. Jiang CC, Xiao GY, Zhang X, et al. Formation and corrosion resistance of a phosphate chemical conversion coating on medium carbon low alloy steel. *New J Chem*. 2016;40(2):1347-53.
31. Simescu F, Idrissi H. *In situ* monitoring of zinc phosphate coating formation on mild steel by acoustic emission technique. *Meas Sci Technol*. 2009;20(5):055702.
32. Kavitha C, Narayanan TS, Ravichandran K, et al. Deposition of zinc-zinc phosphate composite coatings on aluminium by cathodic electrochemical treatment. *Surf Coat Technol*. 2014;258:539-48.
33. Flis J, Tobiyama Y, Shiga C, et al. Behaviour of intact and scratched phosphate coatings on zinc, zinc-nickel and mild steel in dilute sodium phosphate solution. *J Appl Electrochem*. 2002;32(4):401-7.
34. Kumar A, Bholá SK, Majumdar JD. Microstructural characterization and surface properties of zinc phosphated medium carbon low alloy steel. *Surf Coat Technol*. 2012;206(17):3693-9.
35. Banczek EP, Terada M, Rodrigues PR, et al. Effects of niobium ammonium oxalate and benzotriazole on the corrosion resistance of zinc phosphate layer. *J Mater Eng Perform*. 2013;22(11):3572-83.
36. Su HY, Lin CS. Effect of additives on the properties of phosphate conversion coating on electrogalvanized steel sheet. *Corros Sci*. 2014;83:137-46.
37. Cui XJ, Li MT, Yang RS, et al. Structure and properties of a duplex coating combining micro-arc oxidation and baking layer on AZ91D Mg alloy. *Appl Surf Sci*. 2016;363:91-100.
38. Bakhshandeh E, Jannesari A, Ranjbar Z, et al. Anti-corrosion hybrid coatings based on epoxy-silica nanocomposites: Toward relationship between the morphology and EIS data. *Prog Org Coat*. 2014;77(7):1169-83.
39. Duan H, Yan C, Wang F. Effect of electrolyte additives on performance of plasma electrolytic oxidation films formed on magnesium alloy AZ91D. *Electrochim Acta*. 2007;52(11):3785-93.
40. Ghasemi A, Raja VS, Blawert C, et al. Study of the structure and corrosion behavior of PEO coatings on AM50 magnesium alloy by electrochemical impedance spectroscopy. *Surf Coat Technol*. 2008;202(15):3513-8.
41. Dabalà M, Armelao L, Buchberger A, et al. Cerium-based conversion layers on aluminum alloys. *Appl Surf Sci*. 2001;172(3-4):312-22.
42. Blawert C, Heitmann V, Dietzel W, et al. Influence of process parameters on the corrosion properties of electrolytic conversion plasma coated magnesium alloys. *Surf Coat Technol*. 2005;200(1-4):68-72.
43. Hirschorn B, Orazem ME, Tribollet B, et al. Determination of effective capacitance and film thickness from constant-phase-element parameters. *Electrochim Acta*. 2010;55(21):6218-27.
44. Kendig M, Mansfeld F, Tsai S. Determination of the long term corrosion behavior of coated steel with AC impedance measurements. *Corros Sci*. 1983;23(4):317-29.

45. Hosseini MG, Jafari M, Najjar R. Effect of polyaniline-montmorillonite nanocomposite powders addition on corrosion performance of epoxy coatings on Al 5000. *Surf Coat Technol.* 2011;206(2-3):280-6.
46. Ji WG, Hu JM, Zhang JQ, et al. Reducing the water absorption in epoxy coatings by silane monomer incorporation. *Corros Sci.* 2006;48(11):3731-9.
47. Ramezanzadeh B, Vakili H, Amini R. Improved performance of cerium conversion coatings on steel with zinc phosphate post-treatment. *Ind Eng Chem Res.* 2015;30:225-33.